Chemical Engineering Journal 264 (2015) 89–98

Contents lists available at ScienceDirect

Chemical Engineering Journal

journal homepage: www.elsevier.com/locate/cej

Synthesis and characterization of multi-walled carbon nanotubes-supported dibenzo-14-crown-4 ether with proton ionizable carboxyl sidearm as Li^+ adsorbents

Rey Eliseo C. Torrejos [a], Grace M. Nisola [a], Myoung Jun Park [a,c], Ho Kyong Shon [c], Jeong Gil Seo [a], Sangho Koo [a,b], Wook-Jin Chung [a,*]

[a] Energy and Environment Fusion Technology Center (E^2FTC), Department of Energy and Biotechnology (DEB), Myongji University Yongin Science Campus, 449-728, South Korea
[b] Department of Chemistry, Myongji University Yongin Science Campus, 449-728, South Korea
[c] Centre for Technology in Water and Wastewater (CTWW), School of Civil and Environmental Engineering, University of Technology Sydney (UTS), P.O. Box 123, 15 Broadway, NSW 2007, Australia

HIGHLIGHTS

- MWCNT-supported crown ether adsorbents were prepared for Li^+ recovery.
- Synthesis involved MWCNT oxidation, epoxidation, ring opening, and etherification.
- Functionalization steps were verified through several characterization techniques.
- Two MWCNT adsorbents prepared contained: (1) neutral CE and (2) CE with COOH moiety.
- Type (2): better performance, Langmuir-type adsorption, most selective towards Li^+.

ARTICLE INFO

Article history:
Received 2 September 2014
Received in revised form 4 November 2014
Accepted 5 November 2014
Available online 11 November 2014

Keywords:
Adsorbents
Crown ether
Functionalization
Lithium ion recovery
Multi-walled carbon nanotubes
Proton ionizable lariat crown ether

ABSTRACT

A new preparation method for solid-supported crown ethers (CE) as lithium ion (Li^+) adsorbents is presented. Hydroxy-dibenzo-14-crown-4 ether (HDB14C4) was immobilized on multi-walled carbon nanotubes (MWCNTs) through the following steps: (1) MWCNTs were oxidized to generate carboxyl groups (COOH) as functionalization sites for (2) epoxide-terminated linkers. The (3) subsequent epoxide ring opening resulted in the attachment of HDB14C4 and generation of a hydroxyl group in which (4) proton ionizable COOH sidearm was etherified as an optional post CE functionalization step. From this synthesis route, two types of adsorbents were produced: type 1 as MWCNTs with neutral HDB14C4 (steps 1–3) and type 2 as MWCNTs with HDB14C4–COOH sidearm (steps 1–4). Functional group titration and gravimetry revealed that the performed reaction steps efficiently modified the MWCNTs which were strongly supported by FTIR and TGA results. Raman and TEM analyses revealed the preservation of structural integrity of the MWCNTs after functionalization. Between the two materials, the presence of a COOH sidearm in CE of type 2 adsorbent significantly enhanced the Li^+ uptake at pH $\geqslant$7. A Langmuir-type of Li^+ adsorption occurred in type 2 adsorbent. Competitive ion adsorption results revealed that type 2 preferred Li^+ uptake than other metal ions as shown in the sequence: $Li^+ > Na^+ > Mg^{2+} > Ca^{2+}$, K^+, Sr^{2+}. Overall results suggest that the developed synthesis route can effectively produce solid-supported CEs which can be used for precious metal ions recovery.

1. Introduction

The high energy density property of lithium has made it an important component for energy storage devices [1]. Lithium is typically harvested from brine pools via precipitation, but its surging demand has diverted research and commercial interests towards its recovery from alternative resources [1,2]. With extremely low lithium concentration in certain streams such as

* Corresponding author at: Energy and Environment Fusion Technology Center (E^2FTC), Department of Energy and Biotechnology (DEB), Myongji University Yongin Science Campus, 449-728, South Korea. Tel.: +82 31 330 6687; fax: +82 31 337 2902.
E-mail address: wjc0828@gmail.com (W.-J. Chung).

http://dx.doi.org/10.1016/j.cej.2014.11.036
1385-8947/

seawater, industrial and mining wastewater, its recovery would require a simple yet effective process [3,4].

Crown ethers (CE) are known to possess strong affinity towards certain metal ions and their selectivities follow the size-match relation. Complexation is most likely to occur when the ionic size of the metal ion fits well in that of the electron-rich cavity of the CEs. With lithium ion (Li^+) having an ionic diameter of 1.36 Å, 12- to 14-membered CE rings are most selective (cavity size: 1.2–1.5 Å) [5]. Crown ethers have been widely used in catalysis, organic synthesis and sensing [6–9]. However, their employment to sequester metal ions is less popular and if applied, CEs are often integrated in liquid–liquid extraction (LLE) or liquid membrane (LM) systems [10–14]. These processes have low to moderate efficiency, are tedious to perform and utilize toxic organic solvents [15].

With growing interests on materials development for greener processes, CEs in heterogeneous systems have been developed. They can be attached on solid supports or can be polymerized [16–21]. Typically, solid-supported CEs are prepared by attachment of pre-synthesized functionalizable (i.e. hydroxy-terminated) CEs on pre-conditioned surfaces like silica or polymer via etherification. For instance, Li^+-selective crown ether with methylene end was immobilized on hydrophilic polymers by hydroboration oxidation reaction to convert the methylene group to primary hydroxyl (OH) for etherification on polymer supports [20].

Later findings demonstrated the enhanced metal ion uptake and selectivity of CEs in the presence of "built-in" proton ionizable side arm (i.e. carboxyl or COOH groups) [21]. The effect of COOH side groups in CEs has been well demonstrated in LLE and LM systems. But common counter anions, (X^-) which must pair up with Li^+ (i.e. ion pair) for extraction to occur, are often resistant to transport. This predicament often resulted in low Li^+ recoveries. Thus as negatively-charged anion-substitutes, addition of COOH sidearm in CEs promoted Li^+ extraction without the company of a counter-ion. Resins made of polymerized CEs with COOH sidearm for column chromatography application have been prepared previously through condensation with formaldehyde. Although the resin showed high loading and selectivity, the synthesis of CE with COOH was complicated and laborious [21].

As far as it is known, preparation methods for solid-supported CEs with COOH side arms are rarely reported in literature. Furthermore, the most common reaction used for immobilization on solid supports is limited for neutral CEs; etherification of CEs with COOH on solid support could result in undesirable product outcome as the COOH sidearm could react with the oxidizing reagent [16].

Thus herein, a new preparation technique of a solid-supported CE with COOH sidearm as an adsorbent for Li^+ is presented (Fig. 1). A carbon-based material (multi-walled carbon nanotubes or MWCNTs) was used as a solid support of hydroxy-dibenzo-14-crown-4 ether (HDB14C4), the chosen Li^+-selective CE component [6]. MWCNTs have high specific surface area which is favorable for adsorption contact and functionalization of CEs [22–27]. But more importantly, MWCNTs have tunable surface on which oxygenous functional groups (COOH and OH) can be increased up to 8 mmol/g via oxidation [22–28]. With more surface reactive sites, MWCNTs could anchor more CEs which would be beneficial for higher Li^+ uptake. The well-known solid support silica (i.e. fumed, SBA-15, MCM41) has only ~0.2–5 mmol Si-OH/g of functional groups [16,18,21]. On the other hand, polymer supports like polysulfone, poly(vinylbenzyl chloride), poly(VBC-co-acrylamide), poly(vinylbenzyl-chloride-co-acrylamide) and poly (polyglycidyl metacrylate) have low degree of CE functionalizations which limit the metal uptake capacities of the adsorbents [19,20].

With the complication on immobilizing pre-synthesized CE with COOH sidearm, a more convenient approach was developed in the current study wherein the COOH sidearm was formed *in situ* after CE immobilization. This was accomplished by using epoxide-terminated organic linkers [29,30]. Concomitant with HDB14C4 attachment, the epoxide groups are cleaved from which hydroxyl groups are generated at which the COOHs can be attached through an additional reaction. To observe the effect of COOH sidearm on Li^+ uptake, two adsorbents were prepared: type 1 as MWCNTs functionalized with neutral HDB14C4 as the control and type 2 as MWCNTs functionalized with HDB14C4–COOH (Fig. 1). The efficiency of the preparation steps and the properties of the developed adsorbents were confirmed and examined, respectively, through a series of characterization techniques. Adsorption performances of the prepared materials were evaluated in terms of pH effects, initial Li^+ concentration and competitive metal ion adsorption.

2. Experimental

2.1. Materials

The CE HDB14C4 was synthesized according to the procedures described in the literature (Fig. S1) [31,32]. The solid support MWCNTs (>95 wt%, 20–30 nm outer diameter, 0.5–2 μm length, <1.5 wt% ash content) used in this experiment was acquired from Cheap Tubes, Inc. (Brattleboro, USA). The rest of the reagents and solvents used were purchased from Sigma (MO, USA).

2.2. Synthesis of CE-functionalized MWCNTs

Initially, oxidized MWCNTs (MWCNT–COOH) were prepared via sonication of 500 mg vacuum-dried MWCNTs (90 °C, >1 day) dispersed in 1 L HNO_3/H_2SO_4 (1:3) acid solution at 35 °C for up to 12 h. MWCNT–COOH were recovered through centrifugation at 14,000 rpm and then washed several times with deionized water until neutral pH of the supernatant was achieved. MWCNT–COOH was dried *in vacuo* at 90 °C and analyzed for the degree of oxidation as described in Section 2.6.

Epoxidation of MWCNT–COOH was conducted as follows: 1 g MWCNT–COOH was dispersed in 50 mL acetone refluxed at 60 °C for 24 h blanketed with Argon gas, in the presence of 5.5 mmol (0.31 g) KOH and epichlorohydrin (ECH). Reactant ECH was added in 50% molar excess with respect to the measured amount of COOH groups. The product was centrifuged (14,000 rpm) and washed with acetone several times to remove the unreacted residues and finally vacuum-dried to afford the epoxidized MWCNT–COOH or MWCNT–Ep. The degree of reaction was determined through epoxide titration as described in Section 2.6.

2.3. Preparation of type 1 adsorbent: MWCNT–HDB14C4

Functionalization of MWCNT–Ep with HDB14C4 was performed by covalent attachment of the CE on cleaved epoxide rings of MWCNT–Ep. In a 50 mL 1,4 dioxane, HDB14C4 (8 mmol) was initially dissolved followed by the addition of 10 mmol (0.24 g) NaH then refluxed at 100 °C for 3 h under Argon. After which, 1 g of MWCNT–Ep pre-dispersed via sonication (30 min) in 100 mL 1,4-dioxane was added slowly within 1 h. The reaction was refluxed for 7 days, then the purified product was obtained after it was centrifuged (14,000 rpm) and washed several times with 1,4-dioxane, and finally with deionized water. The washed product was vacuum-dried at 90 °C for 48 h to obtain type 1 adsorbent or MWCNT–HDB14C4.

2.4. Preparation of type 2 adsorbent: MWCNT–HDB14C4–COOH

To introduce the COOH sidearm in MWCNT–HDB14C4, a similar method used for the attachment of HDB14C4 onto MWCNT–Ep

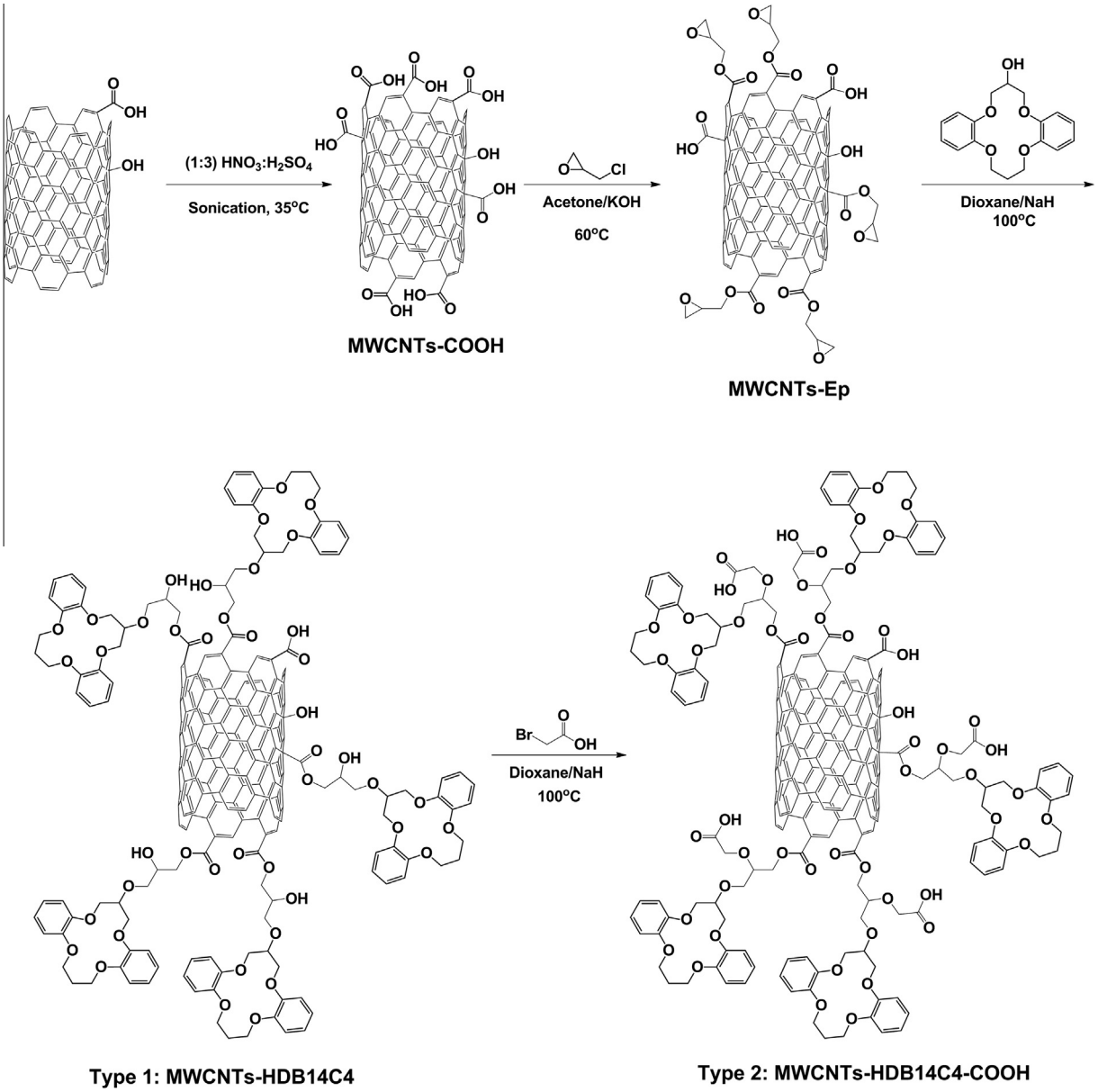

Fig. 1. Synthesis route for the immobilization of HDB14C4 on MWCNTs: step (1) MWCNTs oxidation; step (2) attachment of epoxide-terminated linkers on COOH groups; step (3) attachment of HDB14C4 and generation of free OH group from epoxide ring opening; step (4) etherification for the attachment of COOH sidearm as optional step.

was conducted. The OH groups generated from the cleaved epoxide rings in 1 g of MWCNT–HDB14C4 were etherified with 2.0 mmol (0.28 g) of bromoacetic acid in 1,4-dioxane in the presence of 10 mmol (0.24 g) NaH to finally obtain type 2 adsorbent or MWCNT–HDB14DC4–COOH.

2.5. Extraction experiments

Before use, all adsorbent samples were pre-washed with 0.01 N HCl by vortex mixing and were recovered by centrifugation at 14,000 rpm. The materials were subsequently washed and centrifuged (for recovery) repeatedly with deionized water until neutral pH. The samples were vacuum-dried at 90 °C for at least 48 h and were kept in sealed dry environment when not in use. Unless otherwise stated, all experiments were performed by contacting 25.1 ± 0.10 mg of each type of adsorbent with 2 mL Li^+ containing solutions (i.e. using LiCl or LiOH as salts) for 24 h at room temperature (27 °C). The samples were collected for metal analysis as described in detail in Section 2.6.

For the effect of pH, different Li^+ solutions (0.16 ± 0.02 mM Li^+ from LiCl or LiOH) used were pH-adjusted from 5 to 12. For the effect of Li^+ concentrations, Li^+ solutions (pH = 11.3 ± 0.83 from LiOH and/or LiCl) with concentrations from 0.16 mM to 16 mM were tested. On the other hand, competitive metal ion extraction experiments were performed using a solution containing 0.16 mM Li^+ (from LiCl), 0.14 mM Na^+ (from NaOH), 0.13 mM K^+ (from KCl), 0.12 mM Mg^{2+} (from $MgCl_2$), 0.14 mM Ca^{2+} (from $CaCl_2$) and 0.13 mM Sr^{2+} (from $SrCl_2$).

2.6. Characterization and analytical techniques

The structure of synthesized HDB14C4 was confirmed by ^1H and ^{13}C NMR (Varian, 400 MR Fourier Transform Nuclear Magnetic Resonance) at 400 MHz and 100 MHz, respectively. The degrees of oxidation (MWCNT–COOH), epoxidation (MWCNT–Ep), functionalization with HDB14C4 (MWCNT–HDB14C4), and COOH groups formation on MWCNT–HDB14C4–COOH were quantified through titration or gravimetry. The COOH groups and total number of

acidic groups were quantified through titration using 0.05 M $NaHCO_3$ and 0.05 M NaOH as titrants, respectively. Briefly, 50 mg of pre-dried MWCNT–COOH was stirred in NaOH or $NaHCO_3$. Aliquot was taken and excess NaOH or $NaHCO_3$ was titrated with HCl using methyl red or phenolphthalein as indicators. The amount of OH groups was measured as the difference between the total acid sites and the COOH groups [28,33]. The degree of epoxidation was also determined through titration. The epoxide groups were cleaved by HBr which was produced from the reaction between the excess tetrabutylammonium bromide and perchloric acid as the titrant. The endpoint was achieved with a definite color change using crystal violet as indicator [34].

Gravimetric analysis was specifically performed to quantify HDB14C4 in MWCNT–HDB14C4. For each measurement, at least one gram of dried MWCNT–Ep was carefully weighed and used as MWCNT–HDB14C4 precursor for epoxide ring opening reaction and CE attachment. Prepared MWCNT–HDB14C4 was thoroughly washed with acetone and dioxane, then dried at 80 °C for 12 h. These steps were performed repeatedly for all samples until constant weights were achieved. No sample loss was observed in all materials which were conveniently retrieved via centrifugation at 14,000 rpm. The weights of dried samples were obtained using high precision analytical balance (i.e. four decimal places) and HDB14C4 quantification was obtained as the weight difference before and after the reaction. The reported value was an average of at least three measurements ($n = 3$).

Thermo-gravimetric analysis was performed using Mettler Toledo (DSC823e) TGA analyzer gradually heated from 30 °C to 1000 °C at a rate of 10 °C/min in air, supplied at 100 mL/min. Raman spectroscopy (InVia Reflex UV Raman microscope) with 633 nm He–Ne laser was used to determine the defect densities of the modified MWCNTs. Attenuated total reflectance-fourier transform infrared spectroscopic analysis (ATR-FTIR, Varian 2000) was performed on modified MWCNTs dispersed in methanol to confirm the surface modifications on the MWCNTs. Field Emission Transmission Electron Microscopy (Tecnai F20 FE-TEM) was employed to observe the morphology of the prepared adsorbents. UV–Vis spectrophotometry (Varian Carey 100 Conc) scanned between 200- and 800 nm, was conducted to examine the dispersion property of the adsorbents.

For metal analysis, samples were centrifuged at 14,000 rpm for 10 min to separate the adsorbents. Aliquots of 1 mL supernatant were collected and acid digested with 4 mL DI water and 2 mL concentrated HNO_3 using microwave (MARS 5, CEM Corp.) The final solution was further diluted to 50 mL with deionized water prior to analysis using inductively-coupled plasma mass spectrometry (ICP-MS, Agilent 7500 series, USA).

3. Results and discussion

3.1. Pristine MWCNTs

The as-received MWCNTs feature a clean FTIR spectrum (Fig. 2), without any distinguishable peak, which assures the absence of unwanted artifacts [35]. This was corroborated with the titration analysis wherein no COOH and OH groups were detected (Table 1). The TGA result also supports the FTIR and titration data as no mass loss was observed up to 500 °C (Fig. 3). Complete carbon oxidation took place at 690 °C with 2.5% residue at 800 °C, consistent with those reported in literature [29,36].

3.2. Preparation of MWCNT–COOH via oxidation

For a more functionalizable support, MWCNTs were initially oxidized through sonication in HNO_3/H_2SO_4 acid mixture [36].

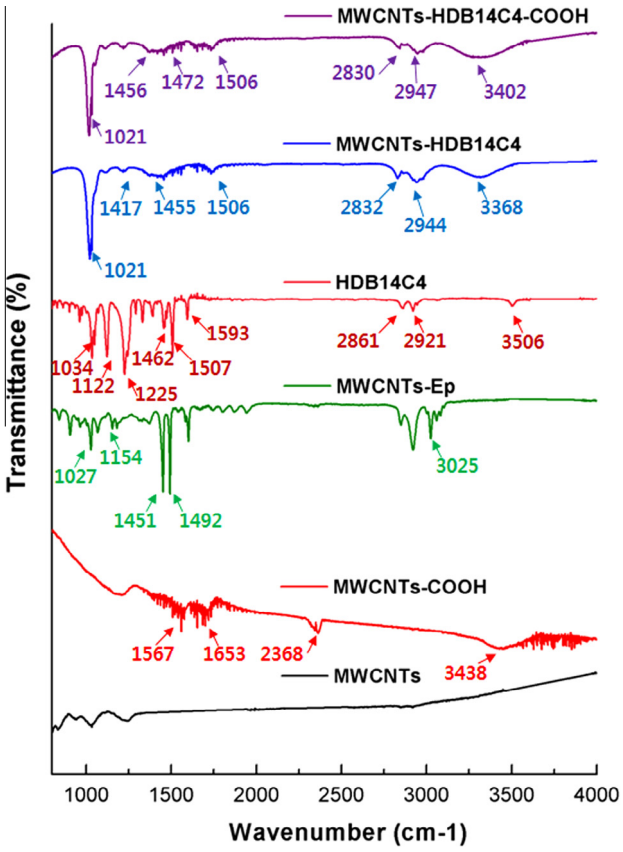

Fig. 2. ATR-FTIR spectra of pristine MWCNTs, modified MWCNTs, HDB14C4 CE and final adsorbent materials (type 1: MWCNT–HDB14C4 and type 2: MWCNT–HDB14C4–COOH).

Table 1
Quantified functional groups on modified MWCNTs.

Synthesis step	Modified MWCNTs (functional groups analyzed)	Quantified functional groups (mmol/g)
	Pristine MWCNTs (COOH)	–
1	MWCNT–COOH (COOH)	5.50[a]
2	MWCNT–Ep (epoxide)	2.00
3	MWCNT–HDB14C4 (HDB14C4)	1.71[b]
4	MWCNT–HDB14C4–COOH (COOH in HDB14C4)	1.33

[a] After 6 h sonication.
[b] Determined via gravimetry (weight difference before and after reaction), all other samples were analyzed via titration.

The method was found effective as ATR-FTIR analysis confirms the presence of characteristic peaks at 3438 cm^{-1} due to the O–H stretch from COOH and OH groups, at 2368 cm^{-1} for the O–H stretch from strongly H-bonded COOH, at 1653 cm^{-1} attributable to C=O stretching of COOH groups and at 1567 cm^{-1} for the carboxylate anion (COO^-) stretch (Fig. 2) [35]. The TGA curve of MWCNT–COOH is also distinguishable from the as-received MWCNT. A mass loss of 3% was observed below 100 °C, due to the release of moisture whereas the gradual mass decline until 620 °C is due to the degradation of COOH and OH groups. Finally, complete decomposition of the nanotubes occurred at 700 °C, with similar residual content as that of pure MWCNTs (Fig. 3).

Sonication time was tuned since it is crucial in maximizing the generation of oxygenous functional groups without compromising the structure of the MWCNTs [33,36]. At the longest sonication

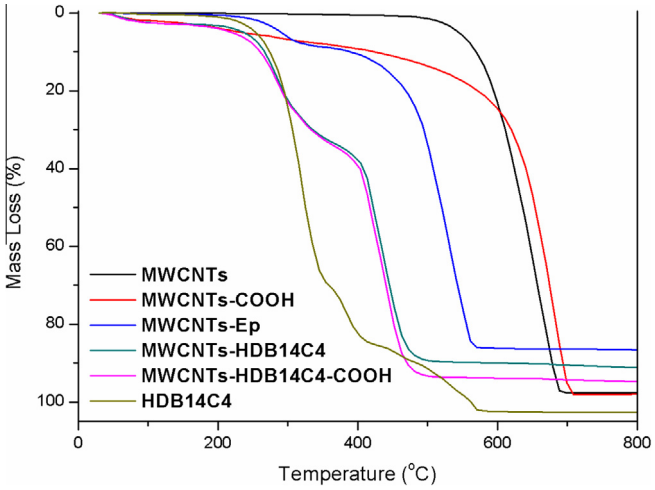

Fig. 3. TGA curves of pure HDB14C4 CE and functionalized MWCNTs.

time (12 h), highest amounts of total acid groups were obtained with 7.11 mmol COOH/g and 2.25 mmol OH/g (Fig. 4). But prolonged sonication resulted in the lowest MWCNT–COOH recovery of 53%. Sonication exacerbated the defects on MWCNTs which resulted in physical disruption and shortening of the nanotubes. The created tube-end defects also became new sites for oxidation. Thus, extended sonication period resulted in (1) reduced size of MWCNT–COOH and (2) increased presence of hydrophilic oxygenous functional groups. Both factors contributed in the decline of MWCNT–COOH recovery.

Considering the trade-off observed between sonication time and material recovery, six-hour sonication was selected as the optimum condition for: (1) the generation of sufficient amounts of COOH (5.5 mmol/g) needed for further functionalization and (2) the retrieval of reasonable amount of MWCNT–COOH.

3.3. MWCNT–Ep synthesis via epoxidation of MWCNT–COOH

With the rich presence of oxygenous groups on MWCNT–COOH, the support can be easily functionalized with CEs per se or CEs with proton ionizable sidearm in the presence of linker molecules. Using

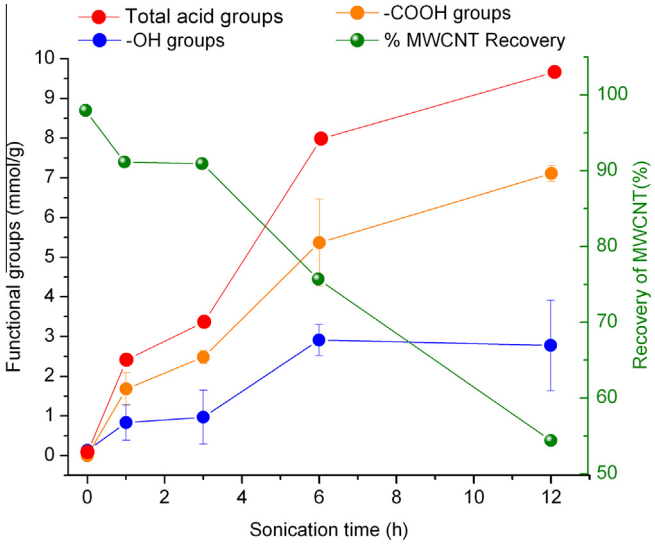

Fig. 4. Effect of sonication time on the degree of oxidation of MWCNTs surface and on its recovery.

the developed immobilization technique, preparation of types 1 and 2 adsorbents was accomplished without the necessity to presynthesize CE–COOH prior to its immobilization. In this technique, an appropriate linker molecule which would only require an additional step to produce COOH sidearm after HDB14C4 immobilization was selected. Epoxides are flexible functional groups which can be readily attacked by nucleophiles (i.e. anionic form of HDB14C4) resulting in its ring opening. One end of the cleaved epoxide would contain the attached CE while the other end would form a free OH group [32,37]. Free OH groups from epoxides can then be further modified to a COOH sidearm to form type 2 adsorbent.

Epoxide groups were incorporated on MWCNT–COOH using ECH in KOH/acetone. The reaction might have proceeded through (1) nucleophilic attack of COO^- (i.e. from deprotonated form of MWCNT–COOH) on the least hindered C of the epoxide ring (chlorohydrin intermediate formation) followed by dehydrohalogenation (ring closure in basic environment) or (2) direct electrophilic substitution at oxygen of COO^- via S_N2 involving the Cl of ECH [38,39]. But in weak base catalyst, the COOH groups have higher propensity to proton loss (COO^-), being more acidic than the OH groups. Hence, majority (if not all) of the epoxide groups might have reacted with the COO^- ions and not with the MWCNTs surface-bound OH groups. Direct titration of epoxide groups reveals that the synthesized MWCNT–Ep contained 2 mmol epoxides/g, suggesting the effectiveness of the performed reaction step (Fig. 1). From this result, it is approximated that 37% of COOH groups on MWCNT–COOH were functionalized with epoxides [30].

ATR-FTIR analysis further confirms the effective formation of MWCNT–Ep as characteristic peaks of O–H stretches from COOH groups at 3438 cm^{-1} and 2368 cm^{-1} disappeared concomitant with the appearance of epoxide C–H stretch at 3025 cm^{-1}, symmetric and asymmetric C–H stretches at 1451-, 1492 cm^{-1} and 1027-, 1154 cm^{-1}, respectively. The TGA analysis of MWCNT–Ep also exhibited a multi-stage decomposition profile. The increasing presence of functional groups on the MWCNTs might have retarded the evacuation and diffusion of decomposing organic molecules [40]. Thus, higher onset of decomposition temperatures was observed at 260 °C and at 440 °C, which can be attributed to the thermal degradation of unreacted COOH- and epoxide groups. Additionally, MWCNT–Ep had higher residual content of 15% than the unmodified MWCNTs and MWCNT–COOH.

3.4. Synthesis of MWCNTs–HDB14C4 (type 1) and MWCNTs–HDB14C4–COOH (type 2)

The CE HDB14C4 was covalently attached on MWCNT–Ep via epoxide ring opening through nucleophilic attack by the deprotonated HDB14C4 using NaH in 1,4-dioxane. Direct epoxide titration of type 1 adsorbent showed no presence of epoxide groups indicating that all were cleaved during the reaction. As complete epoxide ring opening does not accurately equate to the degree of HDB14C4 attachment on MWCNT–Ep, gravimetric quantifications before and after reaction were also performed which revealed the presence of 1.71 mmol HDB14C4/g in type 1 material. This suggests that 86% of the cleaved epoxide rings were successfully functionalized with HDB14C4.

To obtain MWCNT–HDB14C4 with COOH sidearm or type 2 material, COOH groups were incorporated through etherification with bromoacetic acid using NaH as catalyst on the free OH groups formed during ring opening of the epoxide of MWCNT–HDB14C4. Titration results reveal the generation of 1.33 mmol COOH/g, which is equivalent to 78% conversion of type 1 to type 2 adsorbent.

The FTIR spectra of types 1 and 2 adsorbents differ from those of the MWCNT precursors (Fig. 2). However, the two final adsorbents

expectedly have very similar spectra considering their minor functional group difference (i.e. COOH sidearm). The FTIR spectrum of pure HDB14C4 features peaks at: ~3506 cm^{-1} for OH groups, 2921–2861 cm^{-1} for the C=C bridges in the crown ether ring, 1593–1462 cm^{-1} for the aromatic group stretching and 1225–1034 cm^{-1} for the C–O–C ether stretching. In both types 1 and 2 adsorbents, epoxide C–H stretch at 3025 cm^{-1} disappeared which is consistent with the opening of epoxide rings. The strong C–O–C stretch at 1021 cm^{-1} is attributable to the attachment of HDB14C4. Albeit less prominent, the presence of peaks characteristic to HDB14C4 (1417-, 1456- to 1506 cm^{-1} and 2830–2947 cm^{-1}, 2832–2944 cm^{-1}) in the adsorbents further indicates the successful attachment of the CEs. The broad bands at 3368- and 3402 cm^{-1} for the O–H stretch from COOH and OH groups were also present in both materials.

Light absorption properties of MWCNT–HDB14C4 and MWCNT–HDB14C4–COOH were also inspected via UV–Vis spectroscopy in 1:1 (v/v) water/methanol solvent (Fig. 5a). Free HDB14C4 features maximum absorbance peak at λ_{max} = 275 nm, which corresponds to the absorption of aromatic systems in the CE. Similarly, both materials have characteristic peaks but slightly shifted at λ_{max} = 260 nm, which further supports the presence of the CE in both materials.

Types 1 and 2 materials also exhibited similar thermal decomposition patterns (Fig. 3). Both exhibited three stages of thermal degradation. Degradation below 100 °C was due to moisture removal whereas other phases of decomposition started at 240 °C then at 420 °C. The higher mass losses from 240 °C could be due to the larger mass fraction of organics like the CEs present on the MWCNTs, as TGA curve of pure HDB14C4 reveals similar decomposition region from 260 °C to 560 °C. Maximum mass losses were achieved at 480 °C with 11% and 6% residual contents for types 1 and 2, respectively.

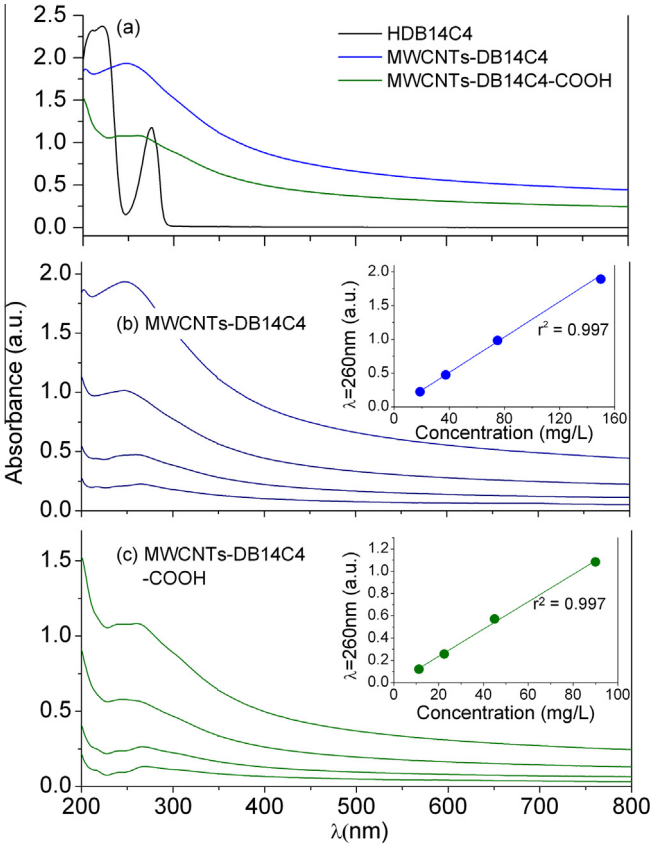

Fig. 5. Optical properties of (a) HDB14C4 and development CE-functionalized MWCNT adsorbents. Absorbance spectra of (b) type 1 and (c) type 2 adsorbents at different dispersion concentrations (Inset in (b) and (c): linear absorbance plots at 260 nm of types 1 and 2 at different adsorbent concentrations) in 1:1 methanol/water solution.

3.5. Structural integrity of the material

The structural integrity of the MWCNTs before and after each modification was determined by Raman spectroscopy (Fig. 6) and TEM analyses (Fig. 7). Raman resonance of unmodified MWCNTs shows two prominent peaks at 1327 and 1580 nm^{-1} for D- and G-band, respectively. The defect mode D-band represents double resonance for amorphous carbon or it can be associated with local defects from structural imperfections of the MWCNTs [41,42]. The graphite mode G-band is related to the tangential in-plane vibration of sp^2 bonded carbons in MWCNTs [36,43]. The integrated intensity (I) ratio (I_D/I_G) was calculated to estimate the defect density in the MWCNTs; I_D/I_G = 1.38 of unmodified MWCNTs was within those reported in literature [41].

Increased I_D/I_G = 1.53 in MWCNT–COOH is consistent with the increase in the defects on the MWCNT walls and edges during oxidation with assisted sonication [41]. But subsequent modifications led to reduction in the defect densities, wherein I_D/I_G values were even lower than the unmodified MWCNTs (Inset Fig. 6). Other studies also observed a decline in I_D/I_G ratio with subsequent functionalization and this was attributed to the gradual removal of carbon debris which was generated during MWCNT oxidation. Likewise, it is an indication that epoxidation, epoxide ring opening and etherification steps did not cause further alteration in the sp^2 bonded carbon networks of the MWCNTs but might have reduced the diffuse Raman active defect sites at the sidewall of the nanotubes [42,44,45]. Thus, the modification steps performed on the MWCNT–COOH proved to be effective for attaching CE while maintaining the structure of the support.

TEM images of the modified MWCNTs (Fig. 7) supported the results of the Raman spectroscopy. The pristine MWCNTs showed highly crystalline structure. But after oxidation, rougher side wall of MWCNT–COOH indicates amorphitization of the nanotube surface along with the formation of COOH and OH groups

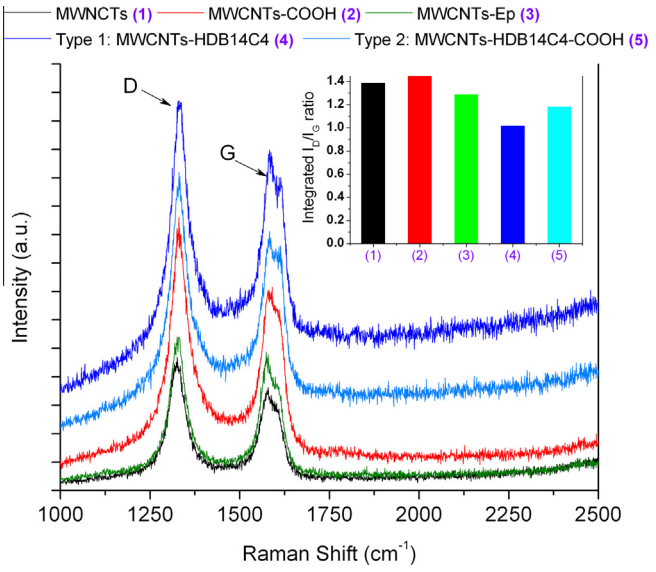

Fig. 6. Raman spectroscopy of pristine MWCNTs, modified MWCNTs and final CE functionalized MWCNT adsorbents (inset: integrated I_G/I_D ratios of the spectra).

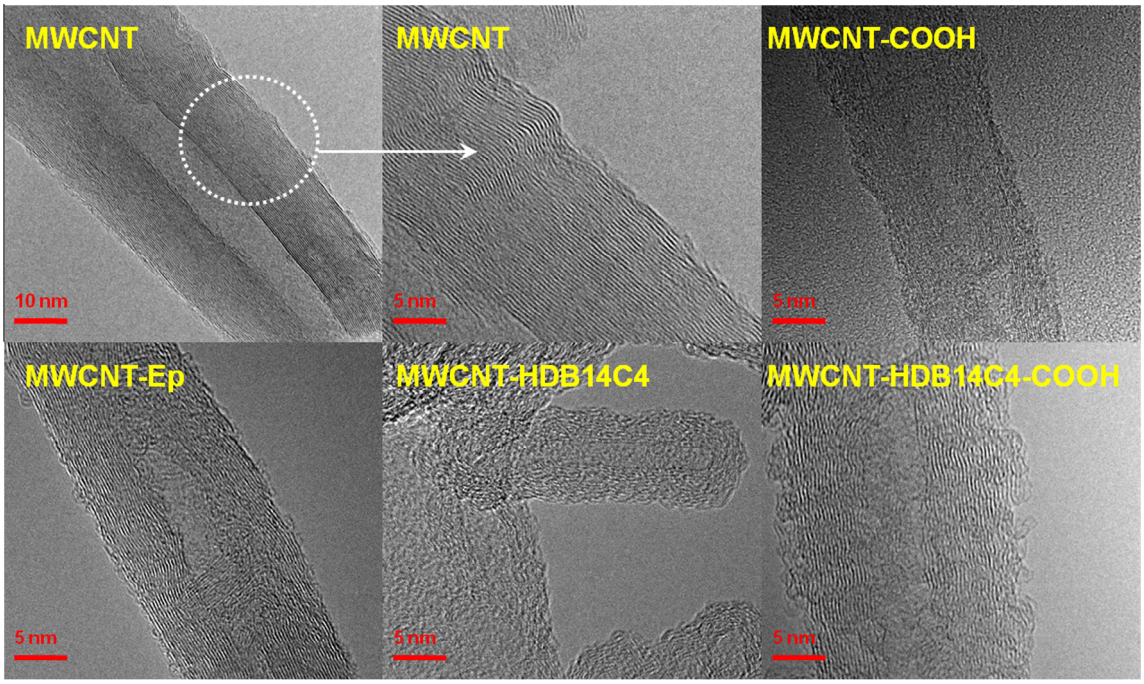

Fig. 7. TEM images of pristine-, modified- and final MWCNT adsorbents.

[41,46]. Further functionalization by epoxidation, immobilization of HDB14C4 and etherification showed amorphous carbon on the surface of the MWCNT, but did not necessarily indicate alteration in the carbon networks of the nanotubes.

3.6. Dispersion of adsorbents in various solvents

The applicability of types 1 and 2 adsorbents in various systems was determined through the quality of their dispersion in different types of solvents. Types 1 and 2 materials were conveniently dispersed in polar (water, methanol, dioxane) solvents and moderately dispersed in non-polar (chloroform, hexane) solvents. Especially in water, suspensions of types 1 and 2 were stable even after 1 month of storage (Fig. S2). The better dispersion of type 2 than type 1 was mainly due to the higher presence of hydrophilic functional groups (i.e. COOH and OH).

The dispersion quality of MWCNT–HDB14C4 and MWCNT–HDB14C4–COOH were also investigated through UV–VIS spectroscopy (Fig. 5b and c). Different concentrations of the modified MWCNTs showed linear absorbance behavior at λ_{max} = 260 nm both having r^2 of 0.997 (Inset: Fig. 5b and c). UV–Vis spectra of both adsorbents at different concentrations followed the Beer–Lambert's law. The high dispersion quality (especially in water) of both adsorbents is favorable for their high contact area with the feed source as it would alleviate transport resistance issues during metal uptake.

On the other hand, retrieval of the adsorbents from the feed water after Li^+ uptake is also an important aspect that must be considered. As a potential application of the developed MWCNT-based adsorbents, the dispersible materials can be incorporated with pre-existing water treatment processes (i.e. in a seawater desalination plant) or can be integrated with a post-treatment step such as a membrane separation unit [4]. The 100% rejection of the adsorbents when passed through a 0.20 μm filter (Supplementary Fig. S3) indicates that micro- or ultrafiltration membranes can be plausibly used for the separation and recovery of the materials from the Li^+-stripped feed source.

3.7. Adsorption performance

To evaluate the ability of the prepared adsorbents for Li^+ sequestration, effects of pH, initial Li^+ concentration as well as the competitive metal ion uptakes were investigated.

3.7.1. Comparison of type 1 and type 2 adsorbents: pH effect

To observe the effect of COOH sidearm on the adsorption performance of HDB14C4-functionalized MWCNT adsorbents, the effect of pH on Li^+ uptake was investigated (Fig. 8). At low pH, both adsorbents exhibited negligible Li^+ uptakes. The proton-rich (H^+) environment at pH = 5.5 has strong influence [1] on the abilities of the adsorbents to sequester cations and [2] on which cation would be preferentially captured. First at low pH, the weak acid carboxylic acid sidearm in type 2 adsorbent might have been in

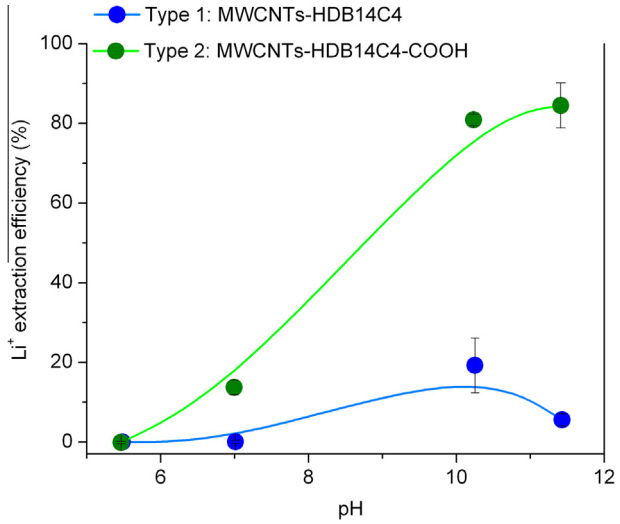

Fig. 8. Li^+ extraction efficiencies of types 1 and 2 adsorbents at different solution pH, [Li^+] = 1 mM.

its un-dissociated form. With the –COOH sidearm having a neutral charge, type 2 would behave similarly with that of type 1. Thus at low pH, both adsorbents would exhibit similar abilities to capture cations which would be solely through cation coordination with HDB14C4. Second, the presence of H^+ in the acidic solution could compete with Li^+ for HDB14C4 complexation. Based on the principle of size-match relation, H^+ which has a smaller ionic diameter (0.74 Å) than Li^+ (1.36 Å) would be preferentially accommodated in the cavity of HDB14C4 [5,47]. Hence at low pH, the negligible Li^+ uptake of both types of adsorbents is mainly due to the favored complexation between the crown ether and H^+ [47].

Contrastingly, both adsorbents demonstrated better Li^+ uptake with pH increase. With proton depletion at basic condition, Li^+ affinity towards the crown ethers is favored hence the improved adsorptions in both materials. The difference in the Li^+ uptakes between types 1 and 2 materials started at pH 7 and the gap became remarkable as the pH was further increased with type 2 material exhibiting a remarkably higher Li^+ uptake than the type 1 adsorbent. The difference can be attributed to the presence of the proton ionizable side arms in type 2 material. At pH $\geqslant$7, these COOH side arms are dissociated into carboxylate anions (COO^-). As more basic moieties, the COO^- side arms in type 2 material provided an extra affinity for the crown ethers, making it easier to capture the Li^+ ions.

A putative mechanism is presented in Fig. 9 to elucidate the Li^+ uptake behaviors of both materials. In type 1, Li^+ uptake is mainly due to its coordination with the neutral electron-rich cavities of HDB14C4. Meanwhile for type 2 adsorbent, the enhanced Li^+ uptake is mainly attributable to the presence of the COOH sidearm with the CE. The ability of weak acid COOH to capture and/or separate metal ions (as COO^-) is well known and has since been well exploited commercially, as cation exchangers [48]. Specifically under basic condition, the strong ion-association interaction between Li^+ and COO^- has been observed in earlier studies [49,50]. It has also been demonstrated that the COO^- sidearm within the proximity of the crown ether assisted in positioning the cation in the CE cavity, which enhanced the cation-CE complexation [21,49,50]. Hence likewise herein, the combined attractive forces from the COO^- sidearm and HDB14C4 in type 2 adsorbent resulted in stronger ion affinity and higher Li^+ uptake. In type 2, the COO^- sidearms also acted as counter-ions for the coordinated Li^+. On par with this, type 1 material recruits available anions (if necessary) in the aqueous stream for this purpose (i.e. Cl^-). With remarkably higher Li^+ uptake performance, further adsorption experiments were conducted using type 2 material.

3.7.2. Li^+ adsorption properties of MWCNT–HDB14C4–COOH

The adsorption capacity of type 2 material was evaluated at different initial Li^+ concentration at pH = 10.5–12.0 using LiOH solution. Within this pH range, adsorption efficiencies are similar as shown in Fig. 8 hence it is assumed that the pH effect would be negligible. The equilibrium adsorption capacity (Q_e) increased with initial Li^+ concentration, achieving the highest value of 5.4 mg/g at the highest Li^+ concentration tested (Fig. 10a). Adsorption results were fitted into linearized Freundlich (Fig. 10b) and Langmuir (Fig. 10c) isotherms expressed in Eqs. (1) and (2), respectively. In Freundlich, K_F is a measure of the adsorptive capacity and $1/n$ pertains to the adsorption intensity of the material whereas q_m is the Langmuir monolayer capacity and K_L is the adsorption binding constant. The Q_e values were plotted against C_e, the equilibrium metal ion concentration [51]. With low linearity in Freundlich equation (r^2 = 0.81), results indicate that the Li^+ adsorption mechanism of type 2 material is well described by the Langmuir model with r^2 = 0.98. Adsorption constants K_L = 0.16 L/g and q_m = 2.11 mg/g were obtained.

$$\ln(Q_e) = \ln(K_F) + \frac{1}{n}\ln(C_e) \quad (1)$$

$$\frac{1}{Q_e} = \frac{1}{K_L q_m}\cdot\frac{1}{C_e} + \frac{1}{q_m} \quad (2)$$

Compared with previously developed solid-supported or polymerized CEs, the q_m of type 2 material is significantly better than the silica-based DB14C4–COOH which reportedly had an uptake

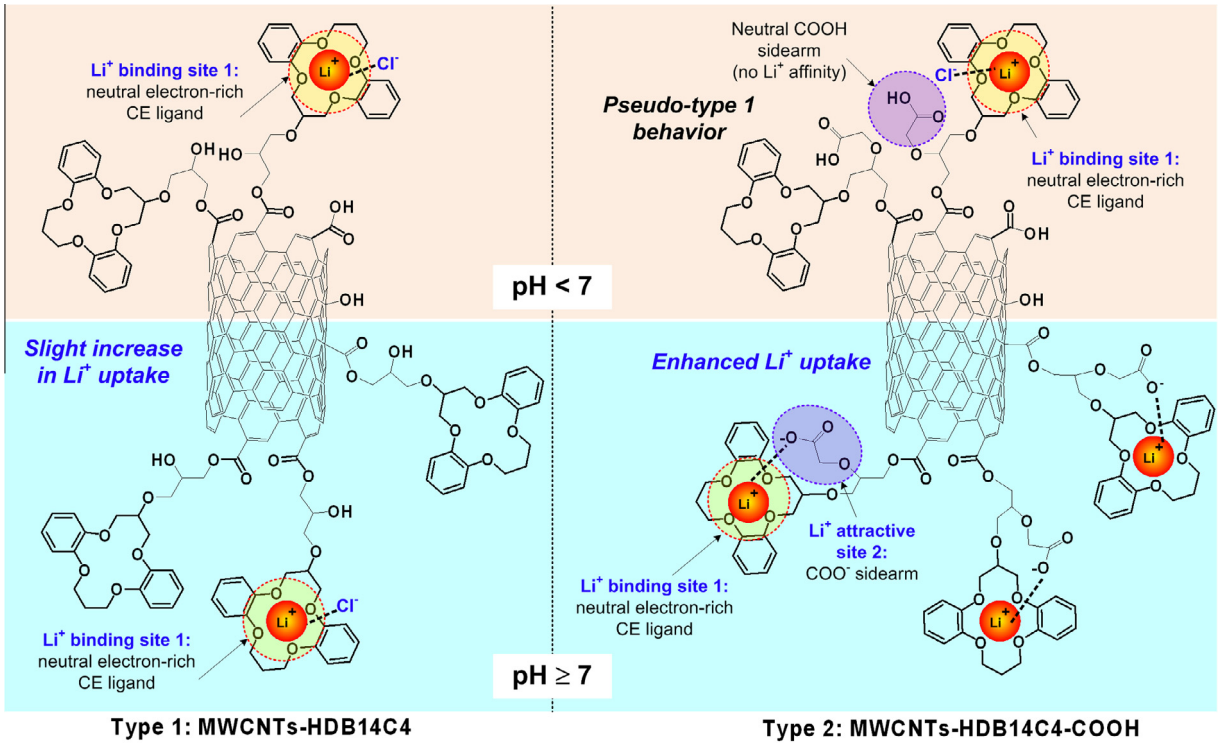

Fig. 9. Mechanism of metal ion-crown ether complex formation in types 1 and 2 adsorbents.

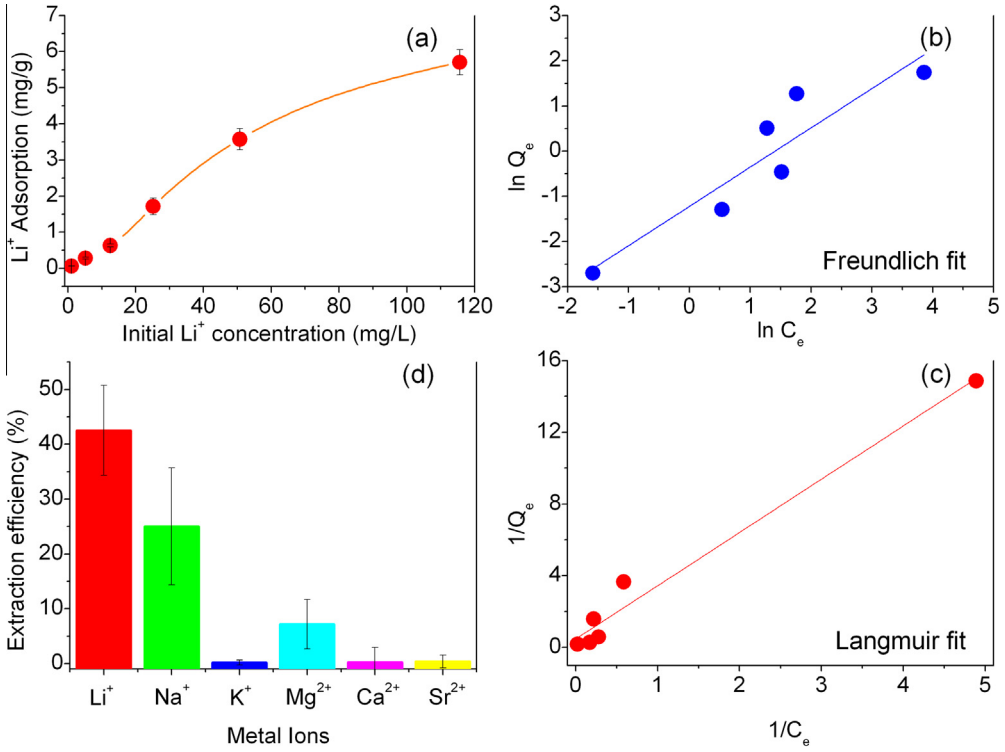

Fig. 10. Adsorption performance of type 2 material (MWCNT–HDB14C4–COOH): (a) Li^+ uptake at different initial concentrations, (b and c) adsorption isotherms, (d) competitive metal ion uptakes.

of 0.05 mg Li^+/g [16]. Its performance is comparable with those of poly(glycidyl-co-ethylene methacrylate)-supported nonamethyl-14C4 (3.05 mg Li^+/g) and polymerized resin of DB14C4–COOH (2.56 mg Li^+/g) [20,21].

In the presence of competing metal ions (Na^+, K^+, Mg^{2+}, Ca^{2+} and Sr^{2+}), the type 2 adsorbent was most selective towards Li^+ (Fig. 10d). It has been reported extensively that HDB14C4 is one of the most selective CEs for Li^+ which follows the size-match relation. The observed uptake of other metal ions could be due to the following reasons: (1) physical retention of other metal ions on the surface of the adsorbent, (2) presence of non-selective adsorption sites (i.e. OH and un-reacted COOH groups) and (3) binding of larger metal ions with crown ethers through 2:1 sandwich type coordination (i.e. Na^+), a phenomenon that has been reported in many studies on CE complexation. Nonetheless, preference for cation uptake of MWCNT–HDB14C4–COOH followed the sequence $Li^+ > Na^+ > Mg^{2+} > Ca^{2+}$, K^+, Sr^{2+}. This trend is an improvement from previously reported solid-supported CEs which often demonstrated poor selectivity towards Li^+. Silica-based DB14C4–COOH demonstrated preference in the following order: $Na^+ > Cs^+ > K^+ \sim Rb^+ > Li^+$ whereas that of polymerized DB14C4–COOH resin preferred Na^+ and K^+ over Li^+ [16,21].

While the current performance of MWCNT–HDB14C4–COOH requires further improvement, the overall finding presented in the current study could be a good benchmark for future development of CE-functionalized solid adsorbents. Specifically, more appropriate CEs can be recruited for better selectivities or novel target-specific CEs can be designed and developed. The findings on the improved Li^+ uptakes in the presence of COOH sidearm with CEs (type 2) further assert the role of proton ionizable groups, not only in LLE systems but also in solid–water interfaces. Surface manipulation of solid supports (i.e. reduction of non-selective binding sites) as well as improvements on the degree of CE functionalization for higher metal ion uptake are also worthy of future investigations.

4. Conclusions

Crown ether functionalized MWCNTs have been successfully prepared and characterized as adsorbents for Li^+ ions. The developed synthetic route was found effective in obtaining the desired adsorbents. Oxidation of MWCNTs provided sufficient functional groups needed for further functionalization. Subsequent reaction steps led to the development of two types of MWCNT adsorbents: type 1 with neutral CE (MWCNT–HDB14C4) and type 2 with COOH proton ionizable side arm in the CE (MWCNT–HDB14C4–COOH). Epoxidation and its subsequent ring opening were critical in simplifying the overall synthetic route as the laborious preparation of HDB14C4–COOH prior to MWCNT functionalization was averted. Type 2 was conveniently synthesized from type 1 via etherification to attach the COOH sidearm. Adsorption results indicate that COOH sidearm in type 2 played a significant role in enhancing the Li^+ uptake. Under basic condition, the deprotonated sidearm (COO^-) provided an extra affinity which made it easier for type 2 to capture the Li^+. Adsorption of Li^+ on type 2 followed the Langmuir isotherm model. In the presence of competing ions, MWCNT–HDB14C4–COOH was most selective towards Li^+.

Acknowledgments

This work was supported by the National Research Foundation of Korea (NRF) grant funded by the Ministry of Science, ICT & Future Planning (No. 2012R1A2A1A01009683) and 2013 Research Fund of Myongji University.

Appendix A. Supplementary data

Supplementary data associated with this article can be found, in the online version, at http://dx.doi.org/10.1016/j.cej.2014.11.036.

References

[1] H. Vikström, S. Davidsson, M. Höök, Lithium availability and future production outlooks, Appl. Energy 110 (2013) 252–266.
[2] L.T. Peiro, G.V. Mendez, R.U. Ayres, Lithium: sources, production, uses and recovery outlook, JOM 65 (2013) 986–996.
[3] R. Chitrakar, H. Kanoh, Y. Miyai, K. Ooi, Recovery of lithium from seawater using manganese oxide adsorbent ($H_{1.6}Mn_{1.6}O_4$) derived from $Li_{1.6}Mn_{1.6}O_4$, Ind. Eng. Chem. Res. 40 (2001) 2054–2058.
[4] M.J. Park, G.M. Nisola, A.B. Beltran, R.E.C. Torrejos, J.G. Seo, S.P. Lee, H. Kim, W.J. Chung, Recyclable composite nanofiber adsorbent for Li^+ recovery from seawater desalination retentate, Chem. Eng. J. 254 (2014) 73–81.
[5] C.J. Pedersen, Cyclic polyethers and their complexes with metal salts, J. Am. Chem. Soc. 89 (1967) 7017–7036.
[6] U. Olsher, The lipophilic macrocyclic polyether 2,3,9,10-dibenzo-1,4,8,11-tetraoxacyclotetradeca-2,9-diene (dibenzo-14-crown-4): a selective ionophore for lithium ions, J. Am. Chem. Soc. 104 (1982) 4006–4007.
[7] H. Sharghi, A.R. Massah, H. Eshghi, K. Niknam, Crown ethers as new catalyst in the highly regioselective halogenative cleavage of epoxides with elemental halogen, J. Org. Chem. 63 (1998) 1455–1461.
[8] G.W. Gokel, W.M. Leevy, M.E. Weber, Crown ethers: sensors for ions and molecular scaffolds for materials and biological models, Chem. Rev. 104 (2004) 2723–2750.
[9] T. Lee, J.W. Chen, H.L. Lee, T.Y. Lin, Y.C. Tsai, S.L. Cheng, S.W. Lee, J.C. Hu, L.T. Chen, Stabilization and spheroidization of ammonium nitrate: co-crystallization with crown ethers and spherical crystallization by solvent screening, Chem. Eng. J. 225 (2013) 809–817.
[10] T.B. Stolwijk, E.J. Sudhoelter, D.N. Reinhoudt, Crown ether mediated transport: a kinetic study of potassium perchlorate transport through a supported liquid membrane containing dibenzo-18-crown-6, J. Am. Chem. Soc. 109 (1987) 7042–7047.
[11] R.A. Bartsch, I.W. Yang, E.G. Jeon, W. Walkowiak, W.A. Charewicz, Selective transport of alkali metal cations in solvent extraction by proton-ionizable dibenzocrown ethers, J. Coord. Chem. 27 (1992) 75–85.
[12] A.E. Visser, R.P. Swatloski, W.M. Reichert, S.T. Griffin, R.D. Rogers, Traditional extractants in nontraditional solvents: group 1 and 2 extraction by crown ethers in room-temperature ionic liquids, Ind. Eng. Chem. Res. 39 (2000) 3596–3604.
[13] S. Tsuchiya, Y. Nakatani, R. Ibrahim, S. Ogawa, Highly efficient separation of lithium chloride from seawater, J. Am. Chem. Soc. 124 (2002) 4936–4937.
[14] R.E.C. Torrejos, G.M. Nisola, M.J. Park, A.B. Beltran, J.G. Seo, S.P. Lee, W.J. Chung, Liquid–liquid extraction of Li^+ using mixed carrier system at room temperature ionic liquid, Desalin. Water Treat. (2014) 1–8.
[15] J.G. Huddleston, H.D. Willauer, R.P. Swatloski, A.E. Visser, R.D. Rogers, Room temperature ionic liquids as novel media for 'clean' liquid–liquid extraction, Chem. Commun. 16 (1998) 1765–1766.
[16] M.G. Hankins, T. Hayashita, S.P. Kasprzyk, R.A. Bartsch, Immobilization of crown ether carboxylic acids on silica gel and their use in column concentration of alkali metal cations from dilute aqueous solution, Anal. Chem. 68 (1996) 2811–2817.
[17] Md.R. Awual, S. Suzuki, T. Taguchi, H. Shiwaku, Y. Okamoto, T. Yaita, Radioactive cesium removal from nuclear wastewater by novel inorganic and conjugate adsorbents, Chem. Eng. J. 242 (2014) 127–135.
[18] W. Qin, S. Xu, G. Xu, Q. Xie, C. Wang, Z. Xu, Preparation of silica gel bound crown ether and its extraction performance towards zirconium and hafnium, Chem. Eng. J. 225 (2013) 528–534.
[19] A. Favre-Reguillon, N. Dumont, B. Dunjic, M. Lemaire, Polymeric and immobilized crown compounds, material for ion separation, Tetrahedron 53 (1997) 1343–1360.
[20] S.D. Alexandratos, C.L. Stine, R.A. Sachleben, B.A. Moyer, Immobilization of lithium-selective 14-crown-4 on crosslinked polymer supports, Polymer 46 (2005) 6347–6352.
[21] T. Hayashita, J.H. Lee, M.G. Hankins, J.C. Lee, J.S. Kim, J.M. Knobeloch, R.A. Bartsch, Selective sorption and column concentration of alkali-metal cations by carboxylic acid resins with dibenzo-14-crown-4 subunits and their acyclic polyether analogues, Anal. Chem. 64 (1992) 815–819.
[22] G.P. Rao, C. Lu, F. Su, Sorption of divalent metal ions from aqueous solution by carbon nanotubes: a review, Sep. Purif. Technol. 58 (2007) 224–231.
[23] D. Tasis, N. Tagmatarchis, A. Bianco, M. Prato, Chemistry of carbon nanotubes, Chem. Rev. 106 (2006) 1105–1136.
[24] M. Holzinger, J. Abraham, P. Whelan, R. Graupner, L. Ley, F. Hennrich, M. Kappes, A. Hirsch, Functionalization of single-walled carbon nanotubes with (R-) oxycarbonyl nitrenes, J. Am. Chem. Soc. 125 (2003) 8566–8580.
[25] G. Kerric, E.J. Parra, G.A. Crespo, F.X. Rius, P. Blondeau, Nanostructured assemblies for ion-sensors: functionalization of multi-wall carbon nanotubes with benzo-18-crown-6 for Pb^{2+} determination, J. Mater. Chem. 22 (2012) 16611–16617.
[26] M.G.C. Kahn, S. Banerjee, S.S. Wong, Solubilization of oxidized single-walled carbon nanotubes in organic and aqueous solvents through organic derivatization, Nano Lett. 2 (2002) 1215–1218.
[27] L. Feng, H. Li, F. Li, Z. Shi, Z. Gu, Functionalization of carbon nanotubes with amphiphilic molecules and their langmuir-blodgett films, Carbon 41 (2003) 2385–2391.
[28] H. Hu, P. Bhowmik, B. Zhao, M.A. Hamon, M.E. Itkis, R.C. Haddon, Determination of the acidic sites of purified single-walled carbon nanotubes by acid-base titration, Chem. Phys. Lett. 345 (2001) 25–28.
[29] F.L. Jin, K.Y. Rhee, S.J. Park, Functionalization of multi-walled carbon nanotubes by epoxide ring-opening polymerization, J. Solid State Chem. 184 (2011) 3253–3256.
[30] A. Eitan, K. Jiang, D. Dukes, R. Andrews, L.S. Schadler, Surface modification of multiwalled carbon nanotubes: toward the tailoring of the interface in polymer composites, Chem. Mater. 15 (2003) 3198–3201.
[31] R.E.C. Torrejos, G.M. Nisola, A.B. Beltran, M.J. Park, B.R. Patil, S.P. Lee, J.G. Seo, W.J. Chung, Microwave-assisted synthesis of dibenzo-crown ethers, Lett. Org. Chem. 11 (2014) 109–115.
[32] G.S. Heo, R.A. Bartsch, L.L. Schlobohm, J.G. Lee, Preparation of hydroxyl crown ethers by reaction of diphenols with epichlorohydrin, J. Org. Chem. 46 (1981) 3575–3576.
[33] A.B. Gonzalez-Guerrero, E. Mendoza, E. Pellicer, F. Alsina, C. Fernandez-Sanchez, L.M. Lechuga, Discriminating the carboxylic groups from the total acidic sites in oxidized multi-walled carbon nanotubes by means of acid-base titration, Chem. Phys. Lett. 462 (2008) 256–259.
[34] R.R. Jay, Direct titration of epoxy compounds and aziridines, Anal. Chem. 36 (1964) 667–668.
[35] F.A. Abuilaiwi, T. Laoui, M. Al-Harthi, M.A. Atieh, Modification and functionalization of multiwalled carbon nanotube (MWCNT) via fischer esterification, Arab. J. Sci. Eng. 35 (2010) 37–48.
[36] V. Datsyuk, M. Kalyva, K. Papagelis, J. Parthenios, D. Tasis, A. Siokou, I. Kallitsis, C. Galiotis, Chemical oxidation of multiwalled carbon nanotubes, Carbon 46 (2008) 833–840.
[37] M.J. Pugia, B.E. Knudsen, C.V. Cason, R.A. Bartsch, Synthesis and alkali-metal complexing abilities of crown ether tertiary alcohols, J. Org. Chem. 52 (1987) 541–547.
[38] A.L. Quintela, M.P. Pellin, S.P. Abuin, Epoxidation reaction of trimethylpropane with epichlorohydrin: kinetic study of chlorohydrin formation, Polym. Eng. Sci. 36 (1996) 568–573.
[39] W. Xiong, Y. Guan, C. Guo, M. Yang, T. Xia, S. Zhao, Preparation of thiourea functionalized polyvinyl alcohol-coated magnetic nanoparticles and their application in Pb^{2+} ions adsorption, J. Appl. Polym. Sci. (2014).
[40] G.M. Nisola, A.B. Beltran, D.M. Sim, D. Lee, B. Jung, W.J. Chung, Dimethyl silane-modified silica in polydimethylsiloxane as gas permeation mixed matrix membrane, J. Polym. Res. 18 (2011) 2415–2424.
[41] S. Osswald, M. Havel, Y. Gogotsi, Monitoring oxidation of multiwalled carbon nanotubes by raman spectroscopy, J. Raman Spectrosc. 38 (2007) 728–736.
[42] G. Grassi, A. Scala, A. Piperno, D. Iannazzo, M. Lanza, C. Milone, A. Pistone, S. Galvagno, A facile and ecofriendly functionalization of multiwalled carbon nanotubes by an old mesoionic compound, Chem. Commun. 48 (2012) 6836–6838.
[43] S. Osswald, E. Flahaut, H. Ye, Y. Gogotsi, Elimination of D-band in raman spectra of double-wall carbon nanotubes by oxidation, Chem. Phys. Lett. 402 (2005) 422–427.
[44] G. Giambastiani, S. Cicchi, A. Giannasi, L. Luconi, A. Rossin, F. Mercuri, C. Bianchini, A. Brandi, M. Melucci, G. Ghini, P. Stagnaro, L. Conzatti, E. Passaglia, M. Zoppi, T. Montini, P. Fornasiero, Functionalization of multiwalled carbon nanotubes with cyclic nitrones for materials and composites: addressing the role of CNT sidewall defects, Chem. Mater. 23 (2011) 1923–1938.
[45] G. Ghini, L. Luconi, A. Rossin, C. Bianchini, G. Giambastiani, S. Cicchi, L. Lascialfari, A. Brandi, A. Giannasi, Can nitrones functionalize carbon nanotubes?, Chem Commun. 46 (2010) 252–254.
[46] R.A. DiLeo, B.J. Landi, R.P. Raffaelle, Purity assessment of multiwalled carbon nanotubes by Raman spectroscopy, J. Appl. Phys. 101 (2007) 064397.
[47] R. Heyrovska, Dependence of the length of hydrogen bond on the covalent and cationic radii of hydrogen, and additivity of bonding distances, Chem. Phys. Lett. 432 (2006) 348–351.
[48] C.E. Harland, Ion Exchange: Theory and Practice, second ed., The Royal Society of Chemistry, Cambridge, 1994.
[49] T. Hayashita, M.J. Goo, J.C. Lee, J.S. Kim, J. Kryzkawski, R.A. Bartsch, Selective sorption of alkali-metal cations by carboxylic acid resins containing acyclic or cyclic polyether units, Anal. Chem. 62 (1990) 2283–2287.
[50] H.P. Gregor, M.J. Hamilton, R.J. Oza, F. Bernstein, Studies on ion exchange resins. XV. Selectivity coefficients of methacrylic acid resins toward alkali metal cations, J. Phys. Chem. 60 (1956) 263–267.
[51] F.O. Okeola, E.O. Odebunmi, Freundlich and Langmuir isotherms parameters for adsorption of methylene blue by activated carbon from agrowastes, Adv. Nat. Appl. Sci. 4 (2010) 281–288.